

Preferential eruption of andesitic magmas through recharge filtering

Adam J. R. Kent^{1*}, Cristina Darr¹, Alison M. Koleszar¹, Morgan J. Salisbury¹ and Kari M. Cooper²

Andesitic volcanic rocks are common in subduction zones and are argued to play an important role in the formation and evolution of the continental crust at convergent margins^{1–4}. Andesite formation is dominated by mixing between iron- and magnesium-rich (mafic) magmas and silica-rich (felsic) magmas^{1,2,4}. The abundance of andesites in many subduction zones suggests they erupt in preference to the magmas that mix to produce them⁴; however, the reasons for this remain unclear. Here we use textural and geochemical analyses of andesites from Mount Hood, Oregon, to show that eruptions are closely linked with episodes of mafic recharge—the intrusion of mafic magma into a shallow felsic magma reservoir. The felsic and mafic magmas involved rarely erupt by themselves, probably because the former are too viscous and the latter too dense. Mafic recharge overcomes these barriers to eruption, and, as it also promotes efficient mixing, results in preferential eruption of mixed andesitic magmas. The abundance of andesites therefore relates to local crustal conditions and the ability of magmas to erupt. We suggest that volcanoes, such as Mount Hood, that erupt homogeneous andesitic compositions through time are those that are the most reliant on mafic recharge to initiate eruptions.

Volcanic rocks provide important information about volcanic and magmatic processes, and the crust and mantle regions where magmas originate. However, to erupt, magmas must overcome physical barriers imposed by density or thermal contrasts between magmas and wall rocks, by high viscosities of crystal and silica-rich magmas and by the stress regime and mechanical strength of the crust. The physical properties that control magma mobility are strongly dependent on composition, and volcanic rocks are thus systematically biased towards eruptible compositions⁵. Previous workers have termed this phenomenon the eruption filter⁵, and we believe it plays an important role in andesite genesis.

In convergent margin volcanics, melt inclusions (representing trapped liquids) with andesitic compositions (~ 58 – 66 wt% SiO₂; this range extends into the dacite field but for simplicity we use the term ‘andesitic’) are significantly less common than more mafic or felsic compositions⁴ (Fig. 1a). However, in terms of bulk magmas, representing the weighted sum of liquid and crystal fractions present, andesitic compositions are considerably more abundant. Although this supports the widespread belief that most andesites form at shallow crustal levels through mixing between mafic and evolved felsic magmas^{1,2,4,6}, it also raises another key question. Why should andesitic volcanic rocks, with compositions produced by mixing, be so common relative to the mafic and felsic magmas that mix to produce them? Andesites are implicated in continental crust growth and evolution³ and associated with significant economic resources and volcanic hazards. A full understanding of their genesis is an important research goal.

We examine andesite petrogenesis with reference to Mount Hood, Oregon, a volcano from the Cascadia subduction zone⁷. Lavas erupted from Mount Hood over the past $\sim 500,000$ years are remarkably restricted in composition, with 95% having SiO₂ contents between 58 and 66 wt% (Fig. 1b,c; Supplementary Table S1), and are also typical of subduction-zone andesites as they are crystal-rich (~ 20 – 45 volume% crystals) and dominated by plagioclase, with lesser amounts of pyroxene, amphibole and oxides^{7–9}. Evidence also suggests that magma mixing plays an important role in petrogenesis at Mount Hood^{2,8–10}: disequilibrium mineral textures and assemblages are ubiquitous, quenched mafic inclusions are common and bulk lava compositions describe simple linear trends on bivariate plots of major oxide composition^{8–10}.

There is particularly strong evidence for two distinct populations of plagioclase related to magma mixing. Crystal-size distributions (CSDs) show a pronounced change in slope at ~ 0.5 mm maximum crystal length (Fig. 2). Such kinked or concave CSDs are commonly considered to result from magma mixing^{11,12}, and this interpretation is supported by differences in plagioclase morphology and composition (Figs 3 and 4; Supplementary Discussion). We refer to plagioclase with maximum crystal lengths between 0.0448 and 0.448 mm as Population 1 and ≥ 0.710 mm as Population 2. Population 1 crystals have euhedral elongate or acicular forms and are normally zoned. Population 2 plagioclase crystals are more tabular in shape, can be glomerocrystic and show highly complex internal textures, including spongy growth zones and internal dissolution surfaces. Population 1 plagioclase crystals have higher and more restricted anorthite and distinctly higher FeO*, MgO, Ti and Sr/Ba than the interiors of the larger Population 2 crystals (Fig. 3, Supplementary Figs S1 and S2). These compositions show that Population 1 crystals formed in equilibrium with relatively mafic melts whereas Population 2 plagioclase formed from evolved felsic melt (Fig. 3).

We can estimate the compositions of magmas that mix to produce erupted andesites, as the bulk lava compositions are strongly correlated with the fraction of Population 1 plagioclase present (Fig. 3). This shows that mixing of mafic and felsic magmas resulted in the juxtaposition of the two different plagioclase populations in their observed proportions and controlled the final erupted lava compositions. As a result extension of the regressions between major element oxides and the fraction of Population 1 plagioclase to 100 and 0% allows us to estimate the bulk compositions of magmas that carried the two crystal populations, and shows that andesites result from mixing between basaltic (50.7 ± 4.3 wt% SiO₂) and rhyolitic (70.9 ± 2.1 wt% SiO₂) magmas (Fig. 2; Supplementary Table S2). Mass balance calculations give equivalent results. Magma mixing at Mount Hood was also highly efficient at the thin-section scale, where plagioclase crystals from each population are intimately intermingled, and at the scale of individual flow units, which are highly homogeneous.

¹Department of Geosciences, Oregon State University, Corvallis, Oregon 97330, USA, ²Department of Geology, University of California at Davis, Davis, California 95616, USA. *e-mail: adam.kent@geo.oregonstate.edu.

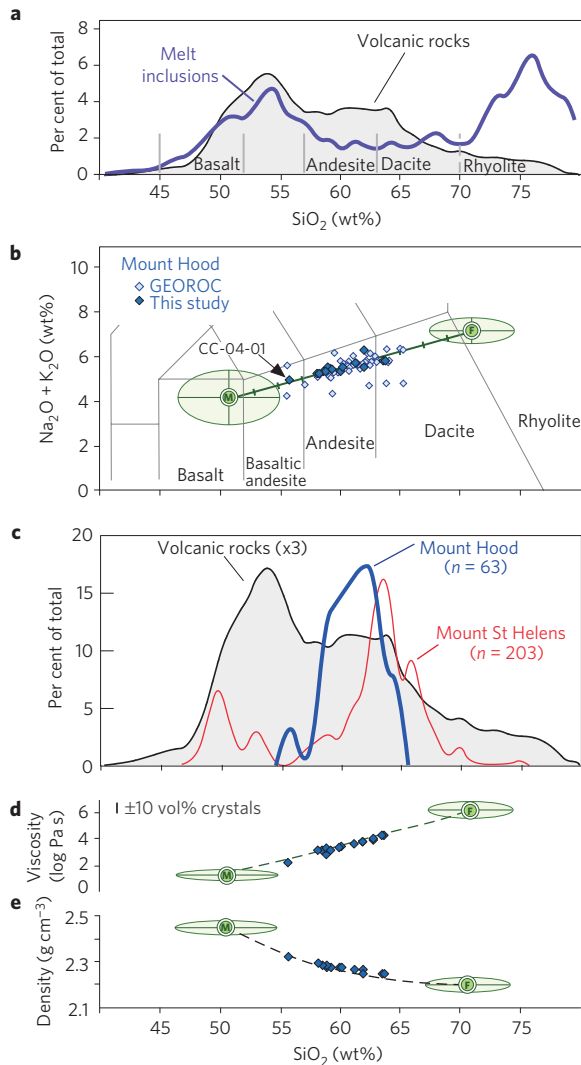


Figure 1 | SiO_2 abundance in melt inclusions and rocks from convergent margin volcanoes and the composition and physical properties of lavas from Mount Hood. **a**, Arc volcanics and melt inclusions⁴. **b**, Total alkalis versus SiO_2 for Mount Hood (this study and GEOROC <http://georoc.mpch-mainz.gwdg.de/georoc/>). Uncertainties are smaller than symbols. Also shown are compositions of mafic and felsic ('M' and 'F') magmas estimated for Mount Hood, with mixing line and ellipses representing uncertainties. **c**, SiO_2 abundance in lavas from Mount Hood, Mount St Helens (from GEOROC) and arc volcanics⁴. **d, e**, Viscosity and density calculated for Mount Hood lavas and mafic and felsic endmember magmas. Ellipses show variations for estimated endmember magmas.

We can assess the timing of magma mixing episodes relative to eruption through mineral zoning. Population 2 plagioclase crystals have narrow rims, $<50\mu\text{m}$ true width, of An_{50-75} plagioclase that are marked by sharp increases in MgO, TiO_2 , FeO^* and anorthite (Fig. 4, Supplementary Fig. S3). We interpret these to represent plagioclase growth following magma mixing. Textural indications of dissolution immediately before rim growth (Fig. 4b,c) are also consistent with transient heating before rim formation. Importantly, the complete absence of high FeO^* (and MgO and TiO_2) in the interiors of Population 2 plagioclase (Fig. 4, Supplementary Fig. S3) shows that mixing of Population 2 plagioclase with more mafic magma occurred only at the very final stage of plagioclase growth, immediately before eruption and cooling, and suggests mixing and eruption are intimately linked. Modelling of the diffusional equilibration of MgO in plagioclase

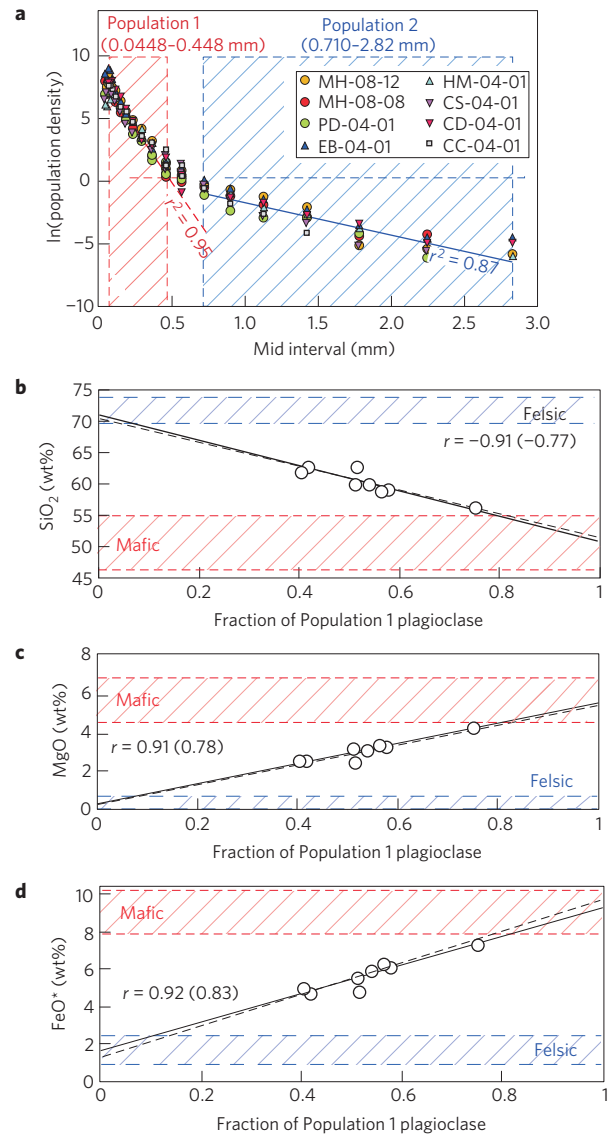


Figure 2 | CSDs and compositions of Mount Hood lavas. **a**, Plagioclase CSDs. The red and blue lines represent best-fit regressions. **b-d**, Correlations between Population 1 proportions and SiO_2 , FeO^* and MgO contents. The red and blue regions show compositions of mafic and felsic endmember magmas estimated by extrapolating regressions to 100 and 0% of Population 1 crystals. Correlation coefficients are given, those in brackets represent regressions without sample CC-04-01, shown as dashed lines. Uncertainties in **a** are smaller than the range of data at a given crystal size. Uncertainties in **b-d** are smaller than the symbol size.

rims confirms this, with calculations showing that Population 2 plagioclase crystals remained at temperatures $\geq 850-900^\circ\text{C}$ for only a few weeks or less following mixing and rim growth (Fig. 4).

Collectively these observations indicate that mafic recharge—introduction of mafic magma to a felsic magma reservoir—is the dominant mechanism by which eruptions are initiated at Mount Hood, and this situation is typical for many subduction-zone volcanoes^{2,6,13-15}. Eruption following recharge results from thermal and volatile exchanges between mixing magmas, changes in volatile solubility, addition of material to a fixed-volume magma chamber and changes in physical properties of the new mixed magma^{1,2,13,14,16,17}. Recharge is also probably most important to eruption in subduction-related magmas, as these are intrinsically volatile-rich².

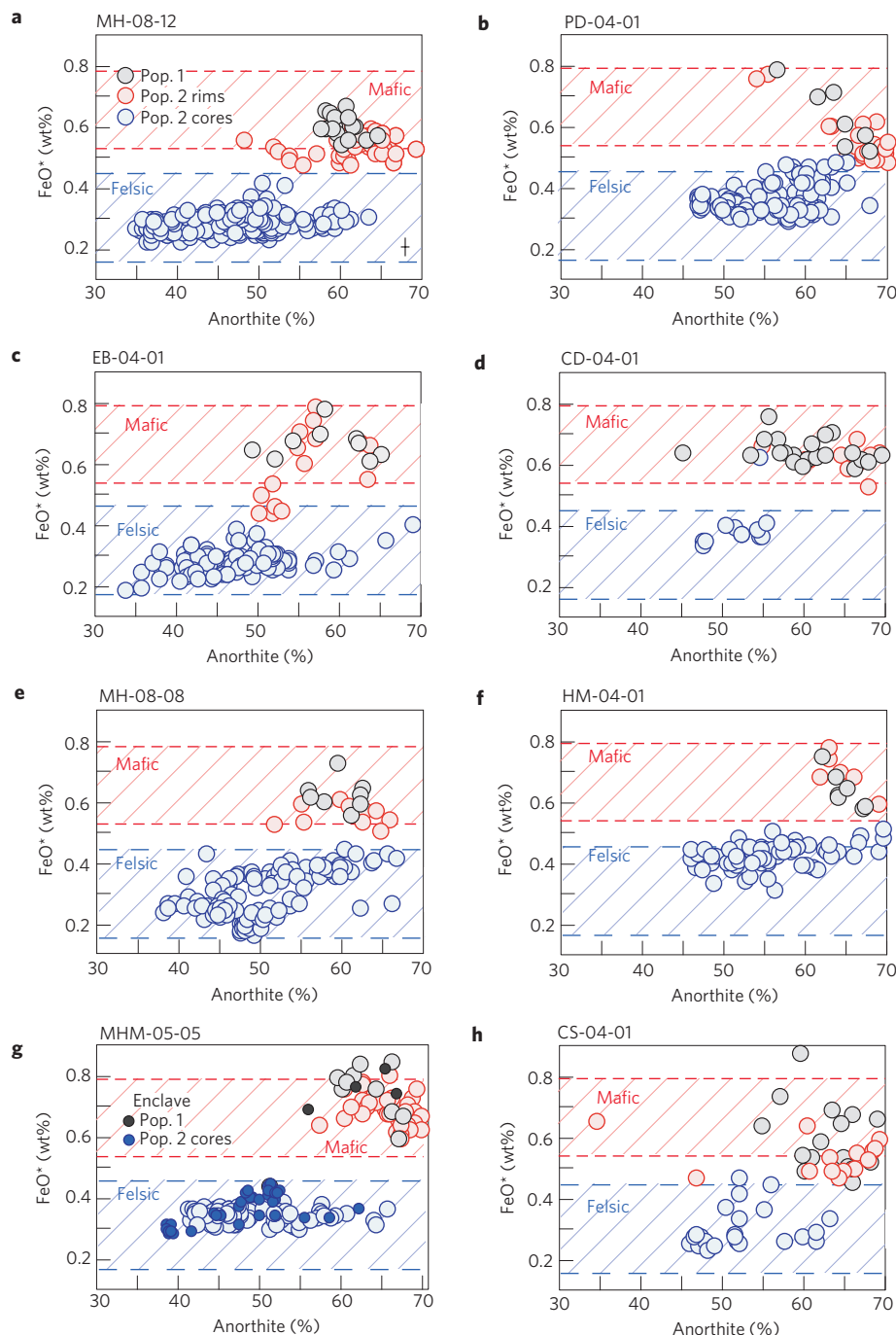


Figure 3 | FeO^* versus anorthite content for plagioclase from Mount Hood lavas. a–h, The grey circles are Population 1 plagioclase, the blue circles represent Population 2 cores and the red circles represent Population 2 rims as described in the text. The red and blue dashed regions represent the expected FeO^* contents of plagioclase crystallized from our estimated mafic and felsic endmember magmas using partition coefficients calculated using ref. 30 and with bulk rock $\text{FeO}/\text{FeO}^* = 0.85$. Compositions of texturally equivalent plagioclase from a mafic enclave are also shown for one sample in **g**. Representative 1 s.d. uncertainties are shown in **a**.

The importance of mafic recharge as an eruption trigger at Mount Hood and elsewhere is also consistent with the presence of significant barriers to eruption of mafic and felsic magmas in many crustal environments. Recharge is one way in which volcanic systems can overcome these barriers and erupt¹³, and results in a fundamental link between mafic recharge, mixing and erupted compositions². Simply put, where mafic recharge is the dominant means by which eruptions are initiated (and where mixing following recharge is efficient), erupted magmas are constrained to have compositions that are intermediate between

those of the mixing magmas. In addition, fluid dynamic constraints further limit efficient mixing to situations where subequal amounts of mafic and felsic magma combine¹⁷. At Mount Hood this results in repeated eruption of magmas that form by late shallow mixing, and that have relatively monotonous andesitic bulk compositions (Fig. 1b,c). Although more mafic and felsic compositions are demonstrably involved in magma genesis, they are unable to consistently erupt. This is probably the result of the high overall viscosity of cool silica-rich felsic magmas, which may also increase rapidly during decompression, and which makes them particularly

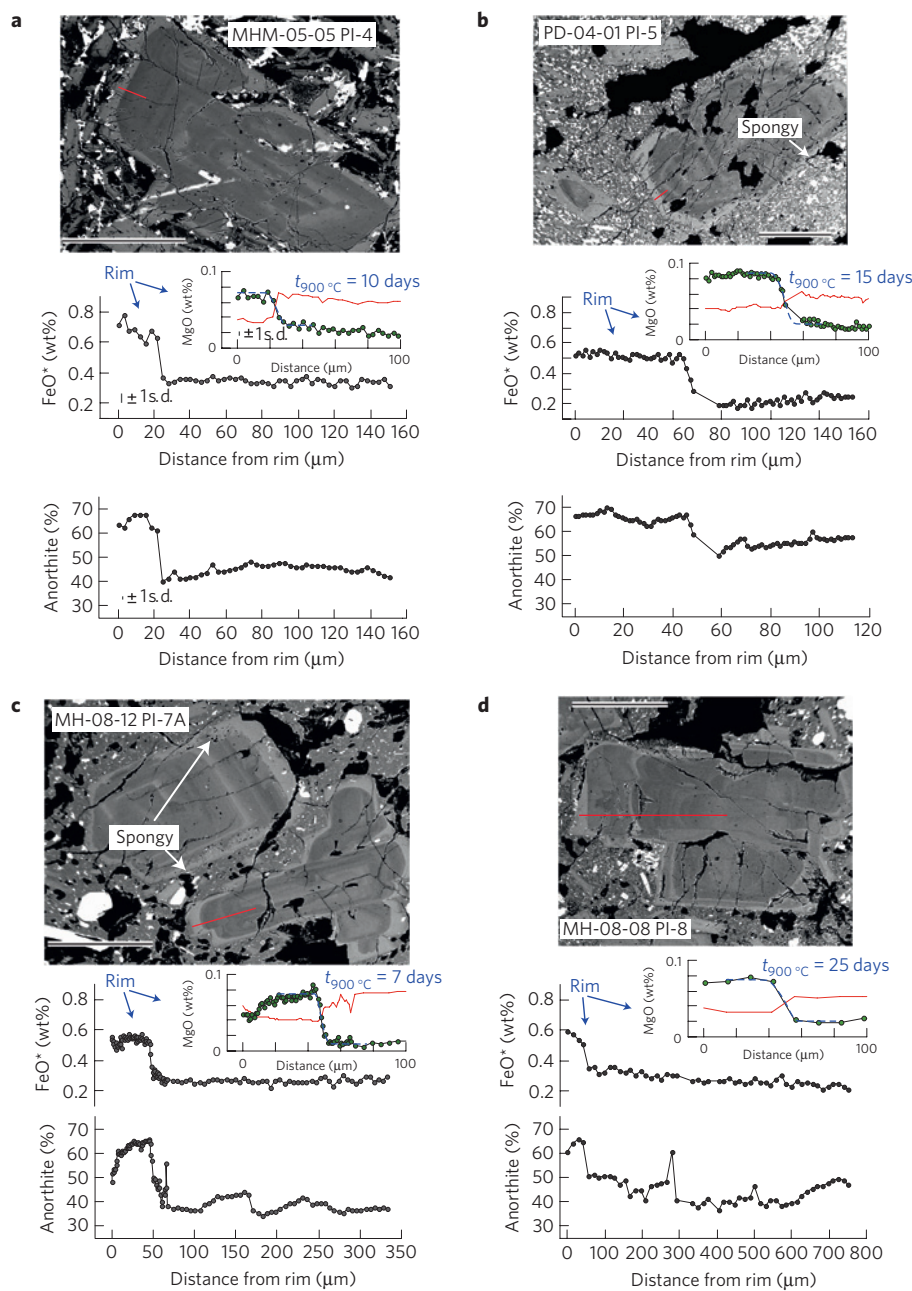


Figure 4 | Backscattered electron images and compositional profiles for selected Population 2 plagioclase from Mount Hood. The scale bar is 500 μm . **a–d**, Compositional traverses show anorthite and FeO^* . The line of each traverse is shown in red. Inset: MgO zoning in the outermost $\sim 100 \mu\text{m}$ (green circles), with the equilibrium MgO distributions shown in red. The blue dashed lines show best-fit 1D diffusion profiles. The estimated time for an initial step function in MgO to decay to the observed data is given in blue text for 900 $^{\circ}\text{C}$. At 850 $^{\circ}\text{C}$ the time required is a factor of ~ 3 longer.

difficult to mobilize^{5,6,16}. Mafic magmas are more fluid, but can be restricted from eruption by their high densities¹⁷, from ‘trapping’ by overpressured felsic magma reservoirs⁶ and by the requirement to maintain sufficiently high temperatures during magma transport^{5,18}. The mobility of any magma is also strongly influenced by the temperature, density, strength and stress field within the surrounding crust, and these can vary on short lateral length scales, and over the life of a volcano in response to edifice growth, magma reservoir conditions and continued magmatism^{6,18}.

Viewed from this perspective, the requirement for mafic recharge to trigger eruptions results in preferential eruption of mixed magmas with intermediate, andesitic, bulk compositions². We term this phenomenon recharge filtering. Andesitic volcanoes that seem to be dominated by recharge filtering are common:

well-characterized examples include Soufrière Hills, Mount Pelée, Mount Unzen and the Plat Pays complex^{15,19–21}. As with Mount Hood, these volcanoes have erupted restricted ranges of broadly andesitic lava compositions over significant time periods ($\geq \sim 10,000$ years), while still showing abundant evidence for mafic recharge and magma mixing, including multiple crystal populations, reverse zoning and the presence of mafic inclusions^{15,19–21}. Given that these petrographic features are common in andesitic volcanics^{1,2}, we suggest recharge filtering is likely to exert a widespread control over volcanic fluxes at convergent margins. Moreover, even where the mixing processes that lead to andesite magma formation do not lead directly to eruption, the physical properties of andesite magmas should still favour their mobility and preferential eruption, as they are less

viscous than the felsic and less dense than the mafic magmas that mix to produce them¹⁷ (Fig. 1). Calculations based on Mount Hood andesites show that these have viscosities between ~2 and 4 log units less than that of the projected felsic magma endmember, and densities about 6–10% lower than the mafic endmember (Fig. 1d).

We expect that volcanoes, such as Mount Hood, that erupt homogeneous andesitic compositions through time are those where crustal barriers to eruption are greatest, and that are thus the most reliant on recharge to initiate eruptions. However, even where crustal conditions allow more diverse lava compositions to erupt, recharge filtering should still exert an important control, simply because of the higher probability of eruption of magmas produced during recharge and mixing. Relative to Mount Hood, Mount St Helens has erupted a relatively diverse array of lava compositions over the past 300,000 years²² (Fig. 1c). Bulk-rock compositions at Mount St Helens range between ~48 and 70 wt% SiO₂, and the significant proportion of lavas with SiO₂ < 55 wt% show that mafic magmas can consistently erupt with little or no mixing with evolved melts (Fig. 1c). However, there is also a peak in abundances at intermediate silica contents (~62–66 wt% SiO₂), and many of these eruptives show abundant petrographic evidence for magma mixing and mafic recharge^{22,23}, suggesting that recharge filtering plays an important, if less dominant, role at this volcano.

The recognition of a widespread role for recharge filtering has important ramifications. Although andesites dominate volcanic outputs at volcanoes such as Mount Hood, they represent magmas produced only at the very final stages of magmatic evolution, and that exist only for very short periods before eruption. Thus, the composition and abundance of andesites may indicate more about local crustal conditions and the ability of magmas to erupt than the conditions of magma generation and long-term storage. Caution is also recommended when using the observed proportions of erupted magmas to infer volumetric proportions within a given melting and magma transport system, unless allowances for recharge filtering or other mechanisms of eruption filtering are taken into account. Finally, the recognition that the predominance of andesitic magmas at convergent margins reflects preferential eruption suggests that the importance of andesites in models for crustal growth and evolution may be overstated.

Methods

Crystal size distributions. Plagioclase CSDs were prepared using the approach detailed in ref. 12. CSDs were based on Al K α compositional maps of Mount Hood lavas made using a Cameca SX-100 electron probe at Oregon State University. Two images were made of each sample, 5 × 5 mm and 20 × 20 mm, enabling CSDs to be determined for a range of crystal sizes. Results from both images were combined to produce a single CSD. Individual plagioclase crystals were outlined by hand in each image and NIH image used to determine best-fit ellipses to approximate the perimeter of each crystal. Crystal lengths were converted from two-dimensional (2D) to 3D with CSDCorrections 1.38 (ref. 24) using a single crystal shape of 1 × 2 × 2 and assuming all grains were unrounded and randomly oriented. Best-fit lines to CSDs were determined using the LINEST least-squares regression procedure in Microsoft Excel. In these lavas, where the groundmass is largely crystalline, consistent differentiation of small microlites (<~50 μ m) was not possible. This may be the reason for the apparent decrease in ln(Population density) at the smallest crystal sizes (<~0.04 mm), and we have used data only for crystals 0.0448 mm or larger for our regressions. To avoid the size region where plagioclase populations overlap, for the purpose of calculating CSD slopes, Population 1 crystals were designated as those with maximum lengths between 0.0448 and 0.448 mm and Population 2 >0.710 mm. To determine the proportions of plagioclase used for Fig. 2b–d, Population 1 and 2 crystals were determined on the basis of the proportion of crystals >0.564 mm (maximum length) being assigned to Population 2. All other crystals (that is, \leq 0.564 mm) were assigned to Population 1.

Diffusion modelling. Diffusion models for MgO in plagioclase shown in Fig. 4 were calculated using the finite-difference approach described in ref. 25. The timescales shown represent the time taken for a perfect step function in Mg concentration to decay to match the observed MgO distribution across the crystal rim, as the crystal approaches equilibrium with the external liquid²⁵. As the

rim–crystal boundary may be gradational initially, and the boundary may not be perfectly normal to the surface of the section, our time estimates should be considered maxima.

Estimation of viscosity and density. The viscosities in Fig. 1d were calculated using the methods outlined in refs 26 and 27. The composition of the liquid fraction present for each sample was estimated by mass balance and removing the observed modal proportions of crystals from each sample, using average mineral compositions. This approach thus assumes that mixing between mafic and felsic magmas resulted in formation of a perfectly mixed liquid. Temperatures of endmember melts were 1,100 °C (mafic) and 800 °C (felsic) and magmas were assumed to have a water content of 4–6 wt%, consistent with preliminary geothermometry and melt inclusion analyses. Magmas were either assumed to have crystallinities equivalent to that measured by CSDs or where that was not measured directly, to vary linearly between 23% crystals and 37% crystals for the mafic and felsic endmembers. Uncertainties reflecting \pm 10 volume% variation in crystallinity are also shown in Fig. 1d and are small relative to the total variation evident. The densities shown in Fig. 1e were calculated using the method of ref. 28. Error ellipses in Fig. 1d,e reflect the variations resulting from uncertainties in the calculated compositions of endmember magmas (Supplementary Table S2).

Major and trace element analyses. Major element and FeO* (denoting total Fe as FeO), TiO₂ and MgO compositions of plagioclase were determined using a Cameca SX-100 electron microprobe at Oregon State University. Analyses were carried out using a 30 nA beam current, with an accelerating voltage of 15 keV, and with a 1 μ m beam diameter. Sodium and K were counted first to reduce volatile loss during analysis and their concentrations were calculated using a zero-time intercept method. Count times range from 20 to 40 s. Standards used for plagioclase calibration include labradorite for Na, Si, Al and Ca, Kakanui augite for Mg, basalt glass for Fe and Ti, and K-feldspar for K. Overall reproducibility estimated from repeat measurement of labradorite was (1 s.d.) \pm 1% (SiO₂, Al₂O₃, Na₂O, CaO), \pm 3% (FeO, MgO), \pm 8% (K₂O) and \pm 13% (TiO₂).

Laser-ablation inductively coupled plasma mass spectrometry analyses were conducted at Oregon State University using the procedures outlined in ref. 29. Typical uncertainties for Sr, Ba and Ti are \pm 5–8% (1 s.d.).

Received 8 March 2010; accepted 2 July 2010; published online 1 August 2010

References

- Anderson, A. T. Magma mixing: Petrological process and volcanological tool. *J. Volcanol. Geotherm. Res.* **1**, 3–33 (1976).
- Eichelberger, J. C. Andesitic volcanism and crustal evolution. *Nature* **275**, 21–27 (1978).
- Rudnick, R. L. Making continental-crust. *Nature* **378**, 571–578 (1995).
- Reubi, O. & Blundy, J. A dearth of intermediate melts at subduction zone volcanoes and the petrogenesis of arc andesites. *Nature* **461**, 1269–1273 (2009).
- Marsh, B. D. On the crystallinity, probability of occurrence, and rheology of lava and magma. *Contrib. Mineral. Petrol.* **78**, 85–98 (1981).
- Eichelberger, J. C., Izbekov, P. E. & Browne, B. L. Bulk chemical trends at arc volcanoes are not liquid lines of descent. *Lithos* **87**, 135–154 (2006).
- Scott, W. E. *et al.* *Geologic History of Mount Hood Volcano, Oregon: A Field-Trip Guidebook* 1–38 (US Geol. Surv. Open File Rep., Vol. 97(263), 1997).
- Cribb, J. W. & Barton, M. Significance of crustal and source region processes on the evolution of compositionally similar calc-alkaline lavas, Mt Hood, Oregon. *J. Volcanol. Geotherm. Res.* **76**, 229–249 (1997).
- Darr, C. M. *Magma Chamber Processes Over the Past 475,000 Years at Mount Hood, Oregon: Insights From Crystal Zoning and Crystal Size Distribution Studies*. M.S. thesis, Oregon State Univ. (2006).
- Woods, M. M. *Compositional and Mineralogical Relationships Between Mafic Inclusions and Host Lavas as Key to Andesite Petrogenesis at Mount Hood Volcano, Oregon*. M.S. thesis, Portland State Univ. (2004).
- Higgins, M. D. & Roberge, J. Three magmatic components in the 1973 eruption of Eldfell volcano, Iceland: Evidence from plagioclase crystal size distribution (CSD) and geochemistry. *J. Volcanol. Geotherm. Res.* **161**, 247–260 (2007).
- Salisbury, M. J., Bohron, W. A., Clynne, M. A., Ramos, F. C. & Hoskin, P. Origin of the 1915 Lassen Peak eruption by magma mixing: Evidence for formation of chemically distinct plagioclase populations from crystal size distributions and *in situ* chemical data. *J. Petrol.* **49**, 1755–1780 (2008).
- Sparks, S. R. J., Sigurdsson, H. & Wilson, L. Magma mixing—mechanism for triggering acid explosive eruptions. *Nature* **267**, 315–318 (1977).
- Eichelberger, J. C. Vesiculation of mafic magma during replenishment of silicic magma reservoirs. *Nature* **288**, 446–450 (1980).
- Murphy, M. D. *et al.* The role of magma mixing in triggering the current eruption at the Soufriere Hills volcano, Montserrat, West Indies. *Geophys. Res. Lett.* **25**, 3433–3436 (1998).
- Watts, R. B., de Silva, S. L., de Rios, G. J. & Croudace, I. Effusive eruption of viscous silicic magma triggered and driven by recharge: A case study of the Cerro Chascon-Runtu Jarita Dome Complex in Southwest Bolivia. *Bull. Volcanol.* **61**, 241–264 (1999).

17. Sparks, R. S. J. & Marshall, L. A. Thermal and mechanical constraints on mixing between mafic and silicic magmas. *J. Volcanol. Geotherm. Res.* **29**, 99–124 (1986).
18. Pinel, V. & Jaupart, C. The effect of edifice load on magma ascent beneath a volcano. *Phil. Trans. R. Soc. Edinburgh* **358**, 1515–1532 (2000).
19. Martel, C., Ali, A. R., Poussineau, S., Gourgaud, A. & Pichavant, M. Basalt-inherited microlites in silicic magmas: Evidence from Mount Pelee (Martinique, French West Indies). *Geology* **34**, 905–908 (2006).
20. Browne, B. L. *et al.* Magma mingling as indicated by texture and Sr/Ba ratios of plagioclase phenocrysts from Unzen volcano, SW Japan. *J. Volcanol. Geotherm. Res.* **154**, 103–116 (2006).
21. Halama, R. *et al.* Pre-eruptive crystallization conditions of mafic and silicic magmas at the Plat Pays volcanic complex, Dominica (Lesser Antilles). *J. Volcanol. Geotherm. Res.* **153**, 200–220 (2006).
22. Clyne, M. A. *et al.* in *A Volcano Rekindled; the Renewed Eruption of Mount St. Helens, 2004–2006*. Vol. 1750 (eds Sherrod, D. R., Scott, W. E. & Stauffer, P. H.) (US Geological Survey Professional Paper, 2008).
23. Pallister, J. S., Hoblitt, R. P., Crandell, D. R. & Mullineaux, D. R. Mount St. Helens a decade after the 1980 eruptions: Magmatic models, chemical cycles, and a revised hazards assessment. *Bull. Volcanol.* **54**, 126–146 (1992).
24. Higgins, M. D. Measurement of crystal size distributions. *Am. Mineral.* **85**, 1105–1116 (2000).
25. Costa, F., Chakraborty, S. & Dohmen, R. Diffusion coupling between trace and major elements and a model for calculation of magma residence times using plagioclase. *Geochim. Cosmochim. Acta* **67**, 2189–2200 (2003).
26. Scaillet, B., Holtz, F. & Pichavant, M. Phase equilibrium constraints on the viscosity of silicic magmas 1. Volcanic–plutonic comparison. *J. Geophys. Res.* **103**, 27257–27266 (1998).
27. Giordano, D., Russell, J. K. & Dingwell, D. B. Viscosity of magmatic liquids: A model. *Earth Planet. Sci. Lett.* **271**, 123–134 (2008).
28. Bottinga, Y. & Weill, D. F. Densities of liquid silicate systems calculated from partial molar volumes of oxide components. *Am. J. Sci.* **269**, 169–182 (1970).
29. Kent, A. J. R. *et al.* Vapor transfer prior to the October 2004 eruption of Mount St Helens, Washington. *Geology* **35**, 231–234 (2007).
30. Lundgaard, K. L. & Tegner, C. Partitioning of ferric and ferrous iron between plagioclase and silicate melt. *Contrib. Mineral. Petrol.* **147**, 470–483 (2004).

Acknowledgements

This research was supported by a grant from the National Science Foundation (EAR-0838421) to A.J.R.K. and K.M.C. and by a USGS Kleinman grant to A.M.K. A.J.R.K. is also grateful for extra support from the University of Aarhus. F. Tepley, A. Weinsteiger and A. Ungerer provided extra assistance with electron microprobe and laser-ablation inductively coupled plasma mass spectrometry analyses. W. Bohrsen provided assistance with CSD measurements and useful discussions. Comments by F. Costa, P. Ruprecht, O. Bachmann, E. Brook, A. Meigs and D. Wildenschild improved an initial version of this manuscript. W. Scott and C. Gardner of the USGS David A. Johnston Cascade Volcano Observatory provided invaluable assistance with sample collection.

Author contributions

C.D. provided initial data from Mount Hood as part of a MS thesis at Oregon State University. C.D. and M.J.S. carried out CSD measurements; A.J.R.K. and A.M.K. obtained mineral chemistry data. A.J.R.K., C.D., A.M.K. and K.M.C. conducted field studies and sampling. All authors provided input to discussion and A.J.R.K. took the lead on writing the manuscript.

Additional information

The authors declare no competing financial interests. Supplementary information accompanies this paper on www.nature.com/naturegeoscience. Reprints and permissions information is available online at <http://npg.nature.com/reprintsandpermissions>. Correspondence and requests for materials should be addressed to A.J.R.K.